



Natural carbazole alkaloid murrayafoline A displays potent anti-neuroinflammatory effect by directly targeting transcription factor Sp1 in LPS-induced microglial cells

Chao-Hua Li, Ying Zhou, Peng-Fei Tu, Ke-Wu Zeng^{*}, Yong Jiang^{*}

State Key Laboratory of Natural and Biomimetic Drugs, School of Pharmaceutical Sciences, Peking University, Beijing 100191, China

ARTICLE INFO

Keywords:

Neuroinflammation
Murrayafoline A (MA)
Specificity protein 1 (Sp1)
Cellular target
NF- κ B

ABSTRACT

Neuroinflammation is a leading cause for neurological disorders. Carbazole alkaloids, isolated from the medicinal plants of *Murraya* species (Rutaceae), have exhibited wide pharmacological activities particularly for neuroinflammation. However, its underlying cellular targets and molecular mechanisms still remain unclear. In current study, we found that murrayafoline A (MA), a carbazole alkaloid obtained from *Murraya tetramera*, potently inhibited the production of neuroinflammation mediators, such as nitric oxide (NO), TNF- α , IL-6 and IL-1 β in LPS-induced BV-2 microglial cells. Then, we performed thermal proteome profiling (TPP) strategy to identify Specificity protein 1 (Sp1) as a potential cellular target of MA. Moreover, we performed surface plasmon resonance (SPR), cellular thermal shift assay (CETSA) and drug affinity responsive target stability (DRATS) assays to confirm the direct interaction between MA and Sp1. Furthermore, we downregulated Sp1 expression in BV2 cells using siRNA transfection, and observed that Sp1 knockdown significantly antagonized MA-mediated inhibition of neuroinflammation mediator production. Meanwhile, Sp1 knockdown also markedly reversed MA-mediated inactivation of IKK β /NF- κ B and p38/JNK MAPKs pathways. Finally, *in vivo* studies revealed that MA significantly suppressed the expression of Iba-1, TNF- α , and IL-6, while increased the number of Nissl bodies in the brains of LPS-induced mice. Taken together, our study demonstrated that MA exerted obvious anti-neuroinflammation effect by directly targeting Sp1, thereby inhibiting NF- κ B and MAPK signaling pathways. Our findings also provided a promising direction of pharmacological targeting Sp1 for anti-neuroinflammation therapeutics as well as novel agent development.

1. Introduction

Specificity protein 1 (Sp1), as a zinc finger family transcription factor, is widely involved in a variety of physiological and pathological processes, including angiogenesis, cell cycle progression, inflammation, and senescence [1-4]. Previous studies have implied that pharmacological regulation of Sp1 exerts potential anti-inflammatory effects in sepsis-induced myocardial injury [5], inflammation related lung injury [6], chronic intestinal inflammation [7], angiotensin II-mediated renal inflammation [8], severe acute pancreatitis [9], and chronic rhinosinusitis [10]. Thus, Sp1 has been considered to be highly associated with inflammation-related diseases.

Recently, several studies have shown that Sp1 over-expression is widely involved in the pathological process of inflammation and neuronal injury, and may play a pivotal role in neuroinflammatory

response [11-13]. For instance, over-expressed Sp1 increased the expression of inflammatory factors, including TNF- α , IL-1 β , and IL-6 in 6-OHDA-induced rat models of Parkinson's disease, while miR-375 attenuated the inflammatory cytokine production by binding to Sp1 3'UTR region [11]. Moreover, it was reported that miR-212-3p weakened Sp1 expression to block beta-site amyloid precursor protein cleaving enzyme 1 (BACE1)-mediated NLRP3/caspase-1 signaling pathway activation, thereby decreasing IL-1 β and IL-18 expression in Alzheimer's disease (AD) rat model and rat hippocampal neuron H19-7 cells [12]. Furthermore, the increased Sp1 could bind on the promoter of miR-183-5p to promote TNF- α , IL-1 β , and IL-6 production in ischemic microglia cell model [13]. Therefore, Sp1 seems to be a highly attractive therapeutic target for neuroinflammation.

The bioactive compounds from medicinal plants have been always explored to search for new therapeutic effects for human diseases

^{*} Corresponding authors.

E-mail addresses: ZKW@bjmu.edu.cn (K.-W. Zeng), yongjiang@bjmu.edu.cn (Y. Jiang).

<https://doi.org/10.1016/j.bioorg.2022.106178>

Received 5 May 2022; Received in revised form 19 September 2022; Accepted 23 September 2022

Available online 28 September 2022

0045-2068/© 2022 Elsevier Inc. All rights reserved.

[14,15]. Carbazole alkaloids, mainly isolated from the *Murraya* species, subfamily Aurantioideae, exhibit a wide variety of biological activities, including antimicrobial effect [16,17], antiprotozoal effect [18,19], anti-inflammation [20,21], antioxidation [22,23], antiplatelet aggregation [24], and anti-HIV activities [25]. Noticeably, midostaurin and carvediol, two typical carbazole alkaloids, have been approved by the FDA for treating tumors and congestive heart failure [26,27]. However, the potential anti-neuroinflammation effect has not been focused previously. Recently, our studies have revealed that some carbazole alkaloids, such as kwangsine M, pyrayaquinone B, and pyrayafoline D6, inhibited NO production in LPS-stimulated BV-2 microglial cells [28], indicating carbazole alkaloids may show potential effect on anti-neuroinflammation therapy. Being similar to the basic skeleton of carbazole alkaloid, murrayafoline A (MA) has been reported to possess various pharmacological activities, including antifungal [29] and anticancer properties [30,31]. However, little is known about its anti-inflammatory activity, especially anti-neuroinflammation, and the underlying mechanisms are still unknown.

In this study, we first explored the potential cellular target and molecular mechanism of MA-mediated anti-neuroinflammatory effect in LPS-induced BV-2 microglial cells. We found that MA directly bound to Sp1 protein and subsequently inhibited the downstream NF- κ B and MAPK signaling pathways. Thus, our study provided new insights into the crucial role of Sp1 as a promising anti-neuroinflammatory target for therapeutic agent development.

2. Materials and methods

2.1. Materials

MA was isolated from *Murraya tetramera* in our group, and its structure was identified as 1-methoxy-3-methylcarbazole by NMR (Fig. S1-2) and ESI-MS data (Fig. S3), and comparison with the reference [32]. Its purity was over 98% detected by HPLC (Fig. S4). Dulbecco's modified Eagle medium and 1% penicillin/streptomycin were purchased from (MACGENE, Beijing, China). Fetal bovine serum (FBS) was purchased from (ABW, Shanghai, China). The primary antibody GAPDH (Cat.No.:60004-1-Ig) was purchased from Proteintech (Chicago, USA) and Sp1 (Cat.No.: ab157123) was purchased from Abcam (Cambridge, England). IkB α (Cat.No.: 4814P), p-IkB α (Cat.No.: 2859T), IKK β (Cat.No.:2370P), p-IKK β (Cat.No.: 2694T), NF- κ B (Cat.No.8242T), p-NF- κ B (Cat.No.:3033T), p38 (Cat.No.:9218P), p-p38 (Cat.No.:4511S), JNK (Cat.No.: 9252T), and p-JNK (Cat.No.: 4668S) were purchased from Cell Signaling Technology (Danvers, MA, USA). The secondary antibody (Cat.No.:BF03015X) was purchased from Biodragon (Suzhou, China). The secondary antibody (Cat.No.: P03S02) was purchased from Gene-Protein Link (Beijing, China).

2.2. Animals

Male Balb/c mice of 6–7 weeks old were obtained from the Department of Laboratory Animal Science (Peking University Health Science Center). All mouse procedures and care were completed in accordance with the protocols approved by the Institutional Animal Care and Use Committee (IACUC) of Peking University Health Science Center, China (Approval Number: LA2019147).

2.3. Cell culture

Murine microglial cell line, BV-2, was purchased from Peking Union Medical College Cell Bank (Beijing, China). The cells were cultured in Dulbecco's Modified Eagle Medium (DMEM, MACGENE, Beijing, China) containing 10% fetal bovine serum (FBS, ABW, Shanghai, China), 100 U/mL penicillin, and 100 μ g/mL streptomycin (MACGENE, Beijing, China) in humidified air containing 5% CO₂ at 37 °C.

2.4. MTT assay

Cell viability was analyzed by using the 3-(4, 5-dimethyl thiazol-2-yl)-2, 5-diphenyl tetrazolium bromide (MTT) assay. Briefly, BV-2 cells were treated with LPS (Sigma-Aldrich, St. Louis, MO, USA) at 1 μ g/mL in the absence or the presence of MA at 5, 10, and 20 μ M for 24 h, respectively. 5 mg/mL of MTT solution (Sigma-Aldrich, St. Louis, MO, USA) was added to the cell culture medium to incubate for 4 h at 37 °C, and then 200 μ L of dimethylsulfoxide (DMSO) was added to dissolve the formazan. Finally, the absorbance at 570 nm was measured using an ELX800 UV universal microplate reader (Bio-Tek, Winooski, VT, USA). Cell viabilities in different groups were normalized to that in control group which was set as 100%.

2.5. Nitric oxide (NO) assay

Nitric oxide (NO) production was quantified by NO assay kit (Applygen, Beijing, China). Briefly, BV-2 cells were treated with LPS at 1 μ g/mL in the absence or the presence of MA at 5, 10, and 20 μ M for 24 h, respectively. Then, the cell supernatant was collected and incubated with Griess reagent at a ratio of 1:1 at room temperature (RT) for 10 min. Finally, the absorbance at 540 nm was detected using ELX800 UV universal microplate reader.

2.6. Enzyme-linked immunosorbent assay (ELISA)

The concentration of inflammatory mediators was detected using Enzyme-linked immunosorbent assay (ELISA). Briefly, BV-2 cells were treated with LPS at 1 μ g/mL in the absence or the presence of MA at 5, 10, and 20 μ M, respectively. Then, the cell supernatant was collected for IL-6 and TNF- α detection using commercial ELISA kits (ExCell Bio Company, Shanghai, China), according to the manufacturer's instruction.

2.7. Quantitative real-time PCR (qRT-PCR)

Total RNA was isolated from vehicle or MA treated BV-2 cells using the RNAPrep Pure Cell/Bacteria Kit (TransGen, Beijing, China) and reverse transcribed using cDNA Synthesis Kit (TransGen, Beijing, China). Quantitative real-time PCR (qRT-PCR) was performed using two-step SYBR green qPCR assays and the target mRNAs were identified by the specific primers. The data were acquired using the Step One™ real time PCR system (Applied Biosystems). The procedure of the target mRNA amplification was as follows: 1 cycle at 95 °C (10 min) followed by 40 cycles at 95 °C (10 s) and 60 °C (30 s). Each assay plate included negative controls with no template. The relative amount of gene expression was analyzed with 2^{- $\Delta\Delta$ Ct} method.

2.8. Thermal proteome profiling (TPP) experiment

Stable isotope labeling BV-2 cells were cultured in DMEM medium with 0.1 mg/mL of ¹³C₆, ¹⁵N₄ Lysine(Lys) and 0.1 mg/mL of ¹³C₆, ¹⁵N₄ Arginine(Arg) (Thermo, San Jose, CA, USA) to replace normal Lys and Arg, respectively. The cells were passed for at least 6 passages until the labeling reach 95% incorporation. The labeled BV-2 cells were treated with LPS at 1 μ g/mL and MA at 20 μ M for 2 h, while non-labeled cells were treated with LPS at 1 μ g/mL and DMSO. After being heated at 65 °C for 3 min, labeled and non-labeled cell lysates were mixed at the ratio of 1:1. Finally, the samples were identified by nanoLC-MS/MS with LTQ-Orbitrap (Thermo, San Jose, CA, USA).

2.9. Surface plasmon resonance (SPR) analysis

The interactions between the proteins and MA were analyzed by Biacore T200 (GE Healthcare, Uppsala, Sweden) at 25 °C. Sp1 protein was dissolved in 10 mM sodium acetate buffer (pH 4.0) immobilized on

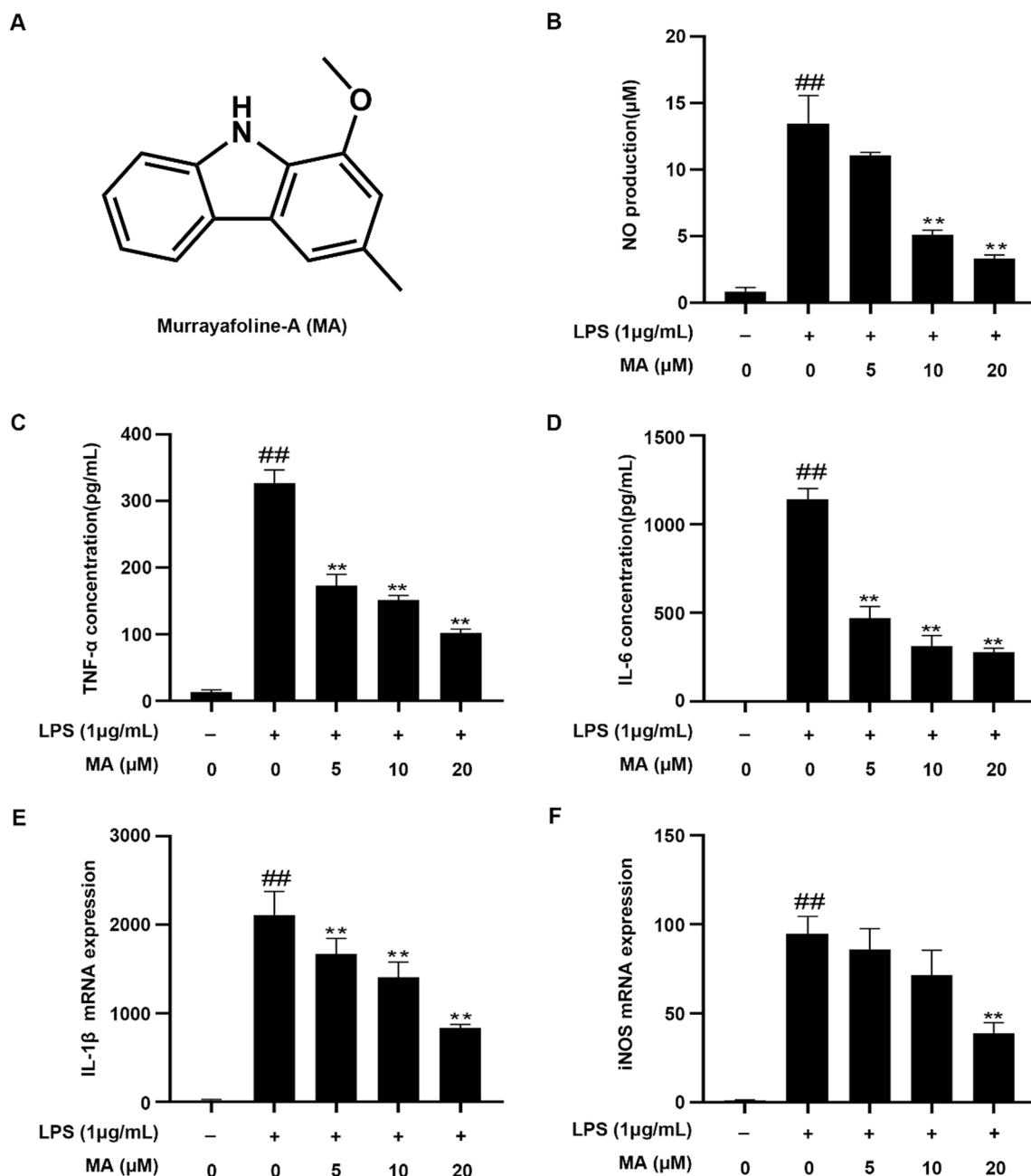


Fig. 1. MA inhibited the inflammatory mediator production in LPS-treated BV-2 cells. (A) The chemical structure of MA. (B–D) MA inhibited LPS-induced NO (B), TNF- α (C), and IL-6 (D) release in BV-2 cells. (E, F) MA inhibited IL-1 β (E) and iNOS (F) mRNA expression in LPS treated BV-2 cells. ^{###} $P < 0.01$ vs. control group. ^{**} $P < 0.01$ vs. LPS group.

CM5 sensor chips. Gradient concentrations of MA in the running buffer ($1.05 \times$ PBS with 5% DMSO and 0.05% tween 20) were added into the CM5 sensor chips, with a flow rate of 30 μ L/min, a contact time of 60 s, and a dissociation time of 120 s. The chip platforms were washed and data were analyzed by using Biacore evaluation software. The curve was fitted with a steady state affinity model for Sp1 with MA in a 1:1 binding model.

2.10. Cellular thermal shift assay (CETSA)

BV-2 cells were respectively treated with MA at 20 μ M and DMSO for 2 h and then aliquoted for heating at different temperatures (40–67 $^{\circ}$ C) for 3 min. Then, the cells were freeze-thawed six times in liquid nitrogen, and the cell lysate was collected for Western blot analysis with indicated antibodies.

2.11. Drug affinity responsive target stability (DARTS) assay

BV-2 cells were treated with MA at 20 μ M for 2 h and then lysed with NP-40 lysis buffer supplemented with 1 mM PMSF. Next, TNC buffer [500 mM Tris-HCl (pH 8.0), 500 mM NaCl, 100 mM CaCl_2] was added, and further incubated with different concentrations of MA for 1 h, followed by addition of 1:8000 pronase (Roche Diagnostics GmbH, Mannheim, Germany) for 20 min at room temperature. Reactions were terminated by boiling for 10 min in $6 \times$ protein loading buffer, and finally analyzed by Western blot with indicated antibodies.

2.12. Fluorescence microscopy

BV-2 cells were plated on 2 cm glass bottom dish at the density of 5×10^5 per dish and incubated in complete DMEM medium overnight. Next

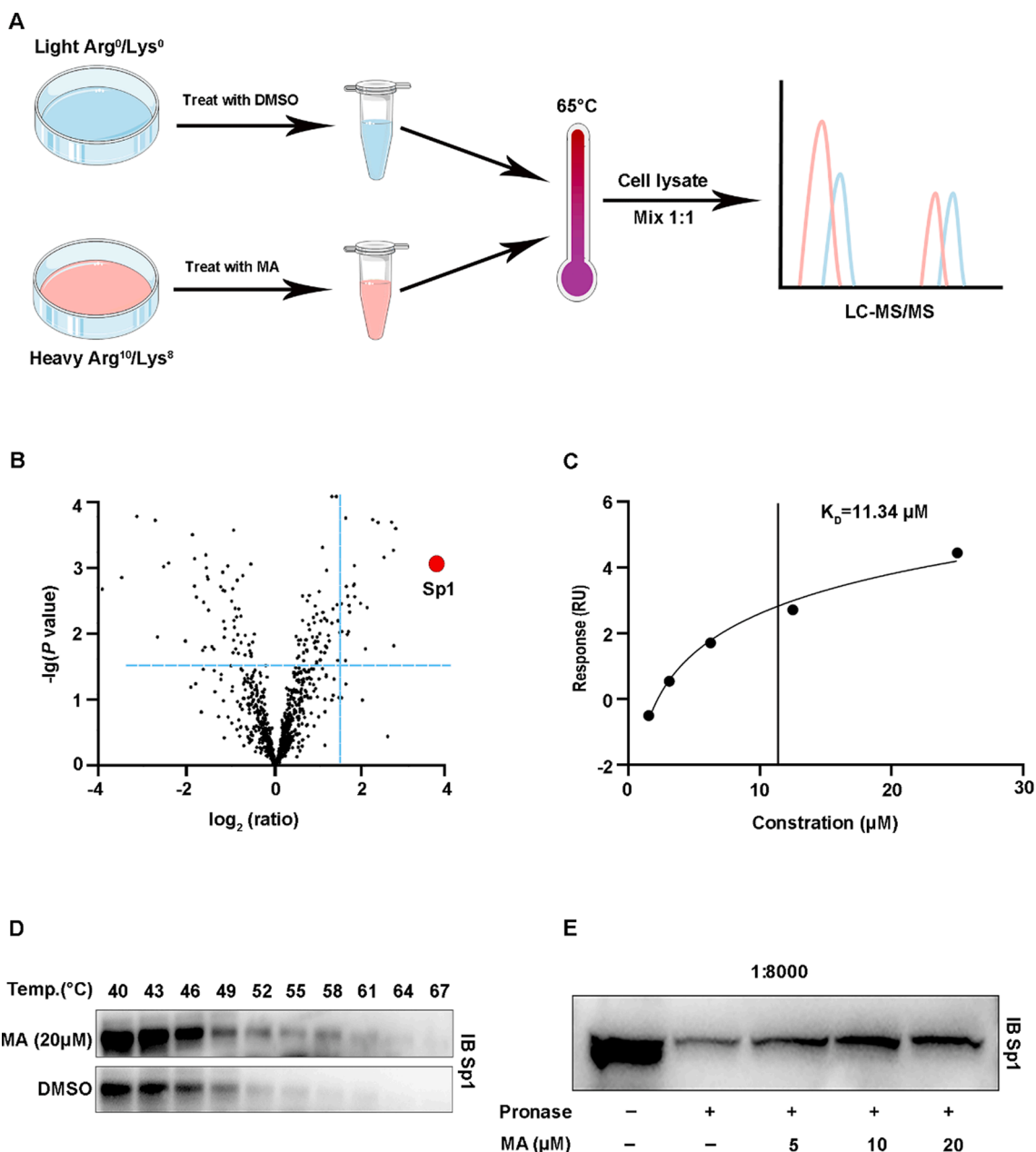


Fig. 2. Sp1 was identified as a cellular target of MA. (A) A schematic identification of MA cellular target by TPP experiment. (B) Light versus heavy isotopic peptide ratios indicated that Sp1 possessed the highest ratio. (C) SPR identified binding affinities of MA with Sp1. (D) CETSA demonstrated stable binding of MA with Sp1. (E) DARTS indicated protease resistance of Sp1 with MA.

day, the cells were treated with or without 1 $\mu\text{g}/\text{mL}$ of LPS in the presence or absence of 20 μM of MA for 6 h. The medium was removed from the dish and the cells were fixed with 4% paraformaldehyde for 20 min. Then, the cells were washed with cold PBS for three times, permeabilized with a solution of 0.5% Triton X-100 for 30 min, washed with cold PBS for three times and blocked with a solution of 5% BSA for 30 min. After incubation with goat polyclonal antibodies to Sp1 (Abcam, Cambridge, England; diluted 1:200) overnight at 4 $^{\circ}\text{C}$, the cells were washed with cold PBS for three times and then incubated with rabbit antibodies to goat (Invitrogen, California, American; red, diluted 1:200) in the dark for 1 h at 37 $^{\circ}\text{C}$. Then, the nuclei were stained with DAPI (Beyotime, Shanghai, China) for 5 min, followed by three washes in cold PBS. Finally, the stained cells were viewed under a fluorescence microscope.

2.13. Transcriptome analysis and bioinformatics analysis

RNA was extracted and target analyses were carried out by the Novogene Company (Beijing, China). RNA integrity and purify were assessed using the RNA Nano 6000 Assay Kit of the Bioanalyzer 2100 system (Agilent Technologies, CA, USA) to explore the targets affected by MA. Pathway analysis on MA was also performed by the Novogene Company. After determining the targets of MA, we used the local version of the Gene Set Enrichment Analysis (GSEA) tool <https://www.broadinstitute.org/gsea/index.jsp>, and GO, KEGG data set were used for GSEA independently. Signal pathways significantly influenced by MA compared with LPS were selected.

2.14. Western blot analysis

After vehicle or MA treatment, BV-2 cells were lysed in ice-cold RIPA

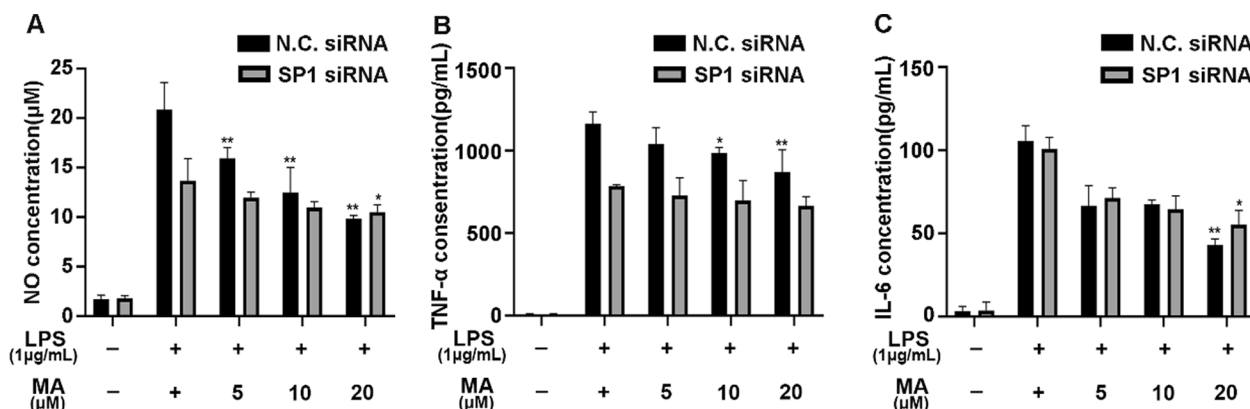


Fig. 3. Sp1 knockdown reversed MA mediated inflammatory mediator inhibition. (A – C) Sp1 siRNA reversed the MA mediated inhibition of NO (A), TNF- α (B), and IL-6 (C) secretion in LPS treated BV-2 cells. * $P < 0.05$, ** $P < 0.01$ vs. LPS group.

buffer containing 1% protease inhibitors (Macgene, Beijing, China). The concentration of total protein was determined by enhanced BCA protein assay reagent (Transgen, Beijing, China). Then, the proteins were separated by 10% sodium dodecyl sulfate-polyacrylamide gel electrophoresis (SDS-PAGE) and transferred onto polyvinylidene fluoride (PVDF) membrane (MERCCK, Darmstadt, Germany). The membranes were then blocked for 1 h in 5% (w/v) skimmed milk solution at room temperature, followed by primary antibodies at 4 °C for night and second antibodies for 1 h at room temperature. Finally, the protein bands were imaged by a Tanon 5200 Imaging Analysis System (Tanon, Shanghai, China). The relative densitometry analysis was carried out by ImageJ software.

2.15. Immunohistochemical assay

Immunohistochemical (IHC) assay was used to detect the activation of microglia in the brain. Brain tissues were collected and fixed in 4% paraformaldehyde, dehydrated in a series of ethanol, and embedded in paraffin. Coronal sections of 5 μm thickness were cut for assay. The slices were deparaffinized and rehydrated, stained with their specific antibodies and imaged using Hamamatsu Nanozoomer (Hamamatsu Photonics, Shizuoka, Japan).

2.16. Nissl staining

Nissl staining was used to detect the morphological changes in the neurons. Brain tissues were fixed in neutral buffered formalin and were dehydrated with different concentrations of ethanol, then embedded with paraffin. After that, the paraffin sections of 5 μm thickness were prepared and then treated with Cresol violet stain solution, followed by washing with running water three times. Then, the sections were dehydrated with different concentrations of ethanol, transparentized in xylene solution and sealed with neutral balsam. Tissues were imaged using Hamamatsu Nanozoomer (Hamamatsu Photonics, Shizuoka, Japan).

2.17. Statistical analysis

All experiments results were presented as means \pm standard deviation (S.D.). Comparisons between groups were conducted using analysis of one-way ANOVA. Statistical analyses were performed in Graph-Pad Prism 7 Software, and p value < 0.05 was considered to be significant.

3. Results

3.1. MA inhibited inflammatory mediator production in LPS-treated BV-2 cells

In order to explore the potential anti-neuroinflammation effect of MA, we treated BV2 cells with LPS in the presence or absence of MA at different levels and then detected the expression of inflammatory factors in the cells. As shown in Fig. 1B, we found that MA (5, 10, 20 μM) significantly inhibited LPS-induced NO production in a concentration-dependent manner. Then, we performed ELISA assay to determine the effect of MA on other inflammatory factor production. We observed that TNF- α and IL-6 expression were significantly increased upon LPS treatment, which was inhibited by MA treatment (5, 10, and 20 μM) in a concentration-dependent manner (Fig. 1C-D). Further, LPS treatment significantly upregulated the mRNA level of IL-1 β , which was markedly decreased by MA treatment (Fig. 1E). Since NO production is induced by inducible nitric oxide synthase (iNOS) catalyzation through inflammatory pathways [33], we then evaluated iNOS gene transcription and found that MA could significantly suppress the iNOS expression at 20 μM (Fig. 1F). In summary, these data indicated a crucial role of MA in attenuating microglia-mediated releases of neuroinflammation mediators.

3.2. Sp1 was a direct cellular target of MA

To map the proteome-wide target proteins of MA, we established thermal proteome profiling (TPP) to analyze the tryptic peptides by LC-MS/MS after a thermal shift assay (Fig. 2A). We first labeled BV2 cells by stable isotope labeling by amino acids in cell culture (SILAC) strategy, and then treated isotopically labeled BV-2 cells with LPS in the presence or absence of MA. As shown in Fig. 2B, the results showed that the highest isotopic ratio was identified as Specificity protein 1 (Sp1). Thereafter, we conducted SPR analysis to demonstrate that the dissociation constant (K_D) of MA binding to Sp1 was 11.34 μM , indicating a specific binding capacity (Fig. 2C). Moreover, CETSA showed that MA increased the stability of Sp1 protein to prevent its temperature-dependent degradation, comparing with the control group (Fig. 2D). Furthermore, DRATS analysis revealed a concentration-dependent reduction of Sp1 proteolysis after incubating with MA (Fig. 2E). The concentration-dependent reduction of Sp1 proteolysis revealed the interaction between MA and Sp1 protein. In sum, these data indicated that Sp1 was a direct cellular target of MA to exert anti-neuroinflammation effect in BV2 cells.

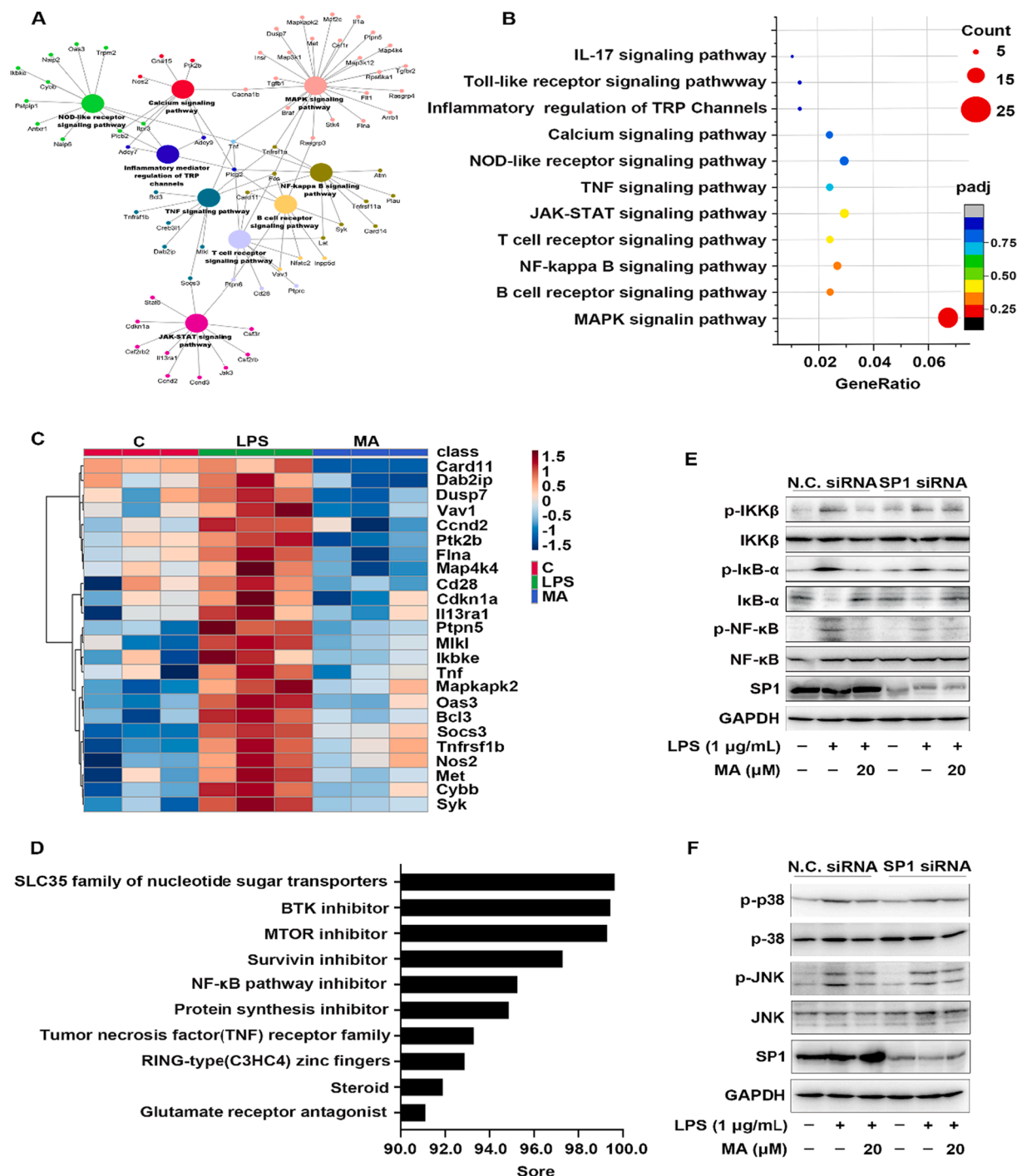


Fig. 4. The mechanism of MA was predicted by transcriptomics combined with bioinformatic analysis. (A) The predicted inflammatory signaling pathways down-regulated by MA were inferred by KEGG assay. (B) The related ratio between MA and inflammatory signaling pathways were inferred by KEGG assay. (C) MA inhibited the expression of related genes in NF- κ B, MAPK, Jak-Stat, B cell receptor, T cell receptor, NOD-like receptor, and calcium signaling pathway. (D) The predicted functions of MA inferred by ConnectivityMap assay. (E, F) MA suppressed Sp1-mediated NF- κ B and MAPK signaling pathway activation.

3.3. Sp1 was necessary for MA-mediated anti-inflammatory activity

To further investigate whether MA exerted anti-neuroinflammation through interaction with Sp1, we firstly performed immunofluorescence analysis to directly visualize the effect of MA on Sp1 protein. The result demonstrated that LPS greatly increased the amount of Sp1 in the nucleus after incubating with BV-2 cells for 6 h, comparing with control group. However, MA significantly down-regulated the amount of Sp1 in the nucleus after treatment for 6 h (Fig. S5). These findings indicated that MA could block Sp1 nuclear translocation and inhibit Sp1 function.

Next, we transfected Sp1-targeting siRNA into BV2 cells, and then detected the inflammatory cytokine expression in the presence or absence of MA upon LPS stimulation. Our results showed that Sp1 siRNA specifically downregulated the Sp1 expression and effectively reversed the MA-mediated inhibition of NO production (Fig. 3A). In addition, the similar reversed effects on TNF- α (Fig. 3B) and IL-6 (Fig. 3C) production were also observed in Sp1 siRNA transfected BV-2 cells. Thus, these dates implied that Sp1 functioned as a main cellular target of MA to exert anti-neuroinflammation effect.

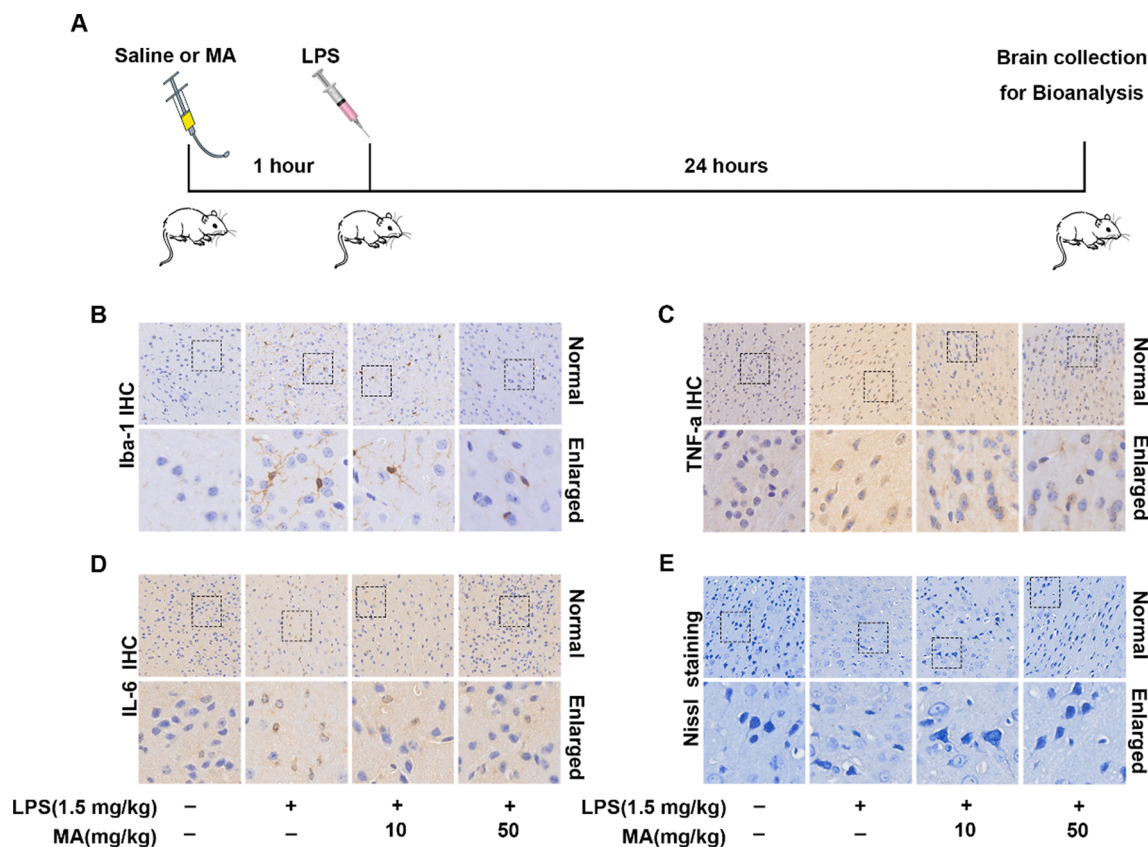


Fig. 5. MA inhibited LPS-induced neuroinflammation *in vivo*. (A) A schematic diagram of animal treatments. (B) MA inhibited microglia activation in the brain of LPS treated C57BL/6 mice by Iba-1 IHC staining. (C-D) MA alleviated the inflammatory mediator release of TNF- α (C) and IL-6 (D) in the brain of LPS treated C57BL/6 mice by IHC staining. (E) MA rescued neuron injury in the brain of LPS treated C57BL/6 mice by Nissl staining.

3.4. MA suppressed Sp1-dependent NF- κ B and MAPK pathway activation

In order to analyze the potential molecular mechanism of the MA mediated anti-inflammatory effect, we performed transcriptomics coupled with bioinformatics analysis to predict the anti-inflammatory signaling pathways of MA in LPS-treated BV-2 cells. The results depicted that 1719 genes, including 908 upregulated genes and 811 down-regulated genes, were significantly changed in MA treated cells. As shown in Fig. 4A, we used KEGG signaling pathway analysis to enrich the inflammation-related genes and obtained nine inflammation-related pathways. Notably, we found that MA mainly regulated MAPK signaling pathway and NF- κ B signaling pathway (Fig. 4B). Next, we used Heatmap, an intuitive visualization method, to further reveal that MA inhibited the expression of NF- κ B pathway-associated Syk, Card11, Tnf genes, and MAPK pathway-associated Dusp7, Flna, Map4k4, Ptpn5, Mapkapk2, Met genes against LPS stimulation (Fig. 4C). In addition, we further predicted biological functions of MA by comparing with the drugs with known biological functions through their common regulated genes on the website of <https://clue.io/>. As shown in Fig. 4D. We found that MA showed similar biological functions with NF- κ B inhibitors among inflammation-related signaling pathways. Furthermore, we detected the total and phosphorylated protein expression of the major mediators in NF- κ B signaling pathway, including IKK β , I κ B α , and NF- κ B, as well as MAPK signaling pathway, including P38 and JNK. The results showed that phosphorylation of IKK β , I κ B α , and NF- κ B was down-regulated by MA, while the downregulations were remarkably reversed after Sp1 knockdown (Fig. 4E). In parallel, Sp1 knockdown also abolished the inhibition of JNK and p38 MAPK phosphorylation by MA (Fig. 4F). Overall, these results suggested that MA attenuated neuroinflammation by suppressing Sp1-dependent NF- κ B and MAPK pathway activation.

3.5. MA attenuated neuroinflammation in LPS-treated Balb/c mice

To further confirm the *in vitro* results, we established LPS-induced inflammation mouse model to evaluate anti-neuroinflammation effect of MA *in vivo* (Fig. 5A). Given ionized calcium-binding adaptor molecule 1 (Iba1) is a marker of microglial activation, we detected the Iba1 expression in the hippocampal and cerebral cortex region. We found that MA administration downregulated LPS-induced Iba1 expression (Fig. 5B), implying that MA prevented LPS induced microglial activation. Then, we analyzed IL-6 and TNF- α expression in the hippocampal and cerebral cortex regions, and found that MA significantly inhibited IL-6 and TNF- α expression upon LPS treatment (Fig. 5C-D), indicating that MA could suppress neuroinflammation *in vivo*. Meanwhile, we performed Nissl staining to evaluate degree of neuronal damage. As shown in Fig. 5E, MA administration effectively protected neurons against microglia-mediated neuroinflammatory injuries by increasing number of Nissl bodies. Overall, these data showed that MA effectively attenuated LPS-induced neuroinflammation *in vivo*.

4. Discussion

In this study, we discovered MA, a simple carbazole, directly bound to Sp1 protein to inhibit LPS-induced neuroinflammation both *in vitro* and *in vivo*. Mechanism study further revealed that the anti-neuroinflammation by MA was attributed to the inhibition of Sp1-mediated NF- κ B and MAPK signaling pathway activation. Our study provides new insights into Sp1 as a promising therapeutic target against neuroinflammation, and MA may serve as a beneficial compound directly targeting Sp1 for anti-neuroinflammation therapy.

As a typical carbazole alkaloid, MA directly targeted Sp1 protein, which was predicted by TPP strategy. Being similar to MA, several

natural products have been reported to target Sp1. For example, curcumin alleviated the levels of inflammatory factors in lung tissues and inflammatory cell infiltration by diminishing Sp1 expression [6]. Besides, synthetic compounds, such as aspirin [34], celecoxib [35], metformin [36], and arsenic trioxide [37], are also involved in Sp1 regulation. For instance, aspirin inhibited cell growth in several colon cancer cells partly via Sp1 inhibition [34]. Moreover, celecoxib repressed migration and invasion of radiation-resistant lung cancer NCI-H1650R cells by inhibiting Sp1 expression [35]. These studies indicated that Sp1 protein was served as a druggable target, while both of natural products and synthetic compounds were rarely reported to participate in anti-neuroinflammation therapy via interaction with Sp1 protein. In current study, we found that MA directly bound to Sp1 protein to inhibit inflammatory mediator production in microglia cells. The direct binding was seldomly reported in anti-neuroinflammation therapy, although previous research had discovered that resveratrol directly bound to Sp1 in MSTO-211H cell lysates to exert anti-tumor effect [38]. In sum, MA was the first reported carbazole alkaloid that directly targeted Sp1 protein, suggesting an insight into traditional medical value of MA in anti-neuroinflammation.

As a pro-inflammatory factor, Sp1, was participated in inflammatory responses in the central nervous system. Inhibition of Sp1 attenuated inflammatory responses and exerted neuroprotection through upregulation of some microRNA, such as miR-375 [11] and miRNA-212-3p [12]. Whereas, it is little known about the natural drugs, which could target Sp1 to inhibit neuroinflammation. Although it has been reported that some natural drugs targeted Sp1 protein in cancers [39,40], we first reported MA inhibited neuroinflammation by targeting Sp1-mediated NF- κ B and MAPK signaling pathways. As reported, Sp1 protein could get involved in many inflammatory signaling pathways. For example, the Sp1-TGF- β 1/Smad3-NF- κ B signaling pathway mediated renal fibrosis and inflammation triggered by angiotensin II infusion [8] and Sp1-HMGB1-NF- κ B signaling axis triggered myocardial dysfunction and inflammation in LPS-induced SIMD (sepsis-induced myocardial dysfunction) mouse model [41]. Moreover, Sp1 was also participated in TLR4-Akt signaling pathway to promote inflammation in THP-1 monocytes [42]. Comparing with the previous studies, our study showed that MA played a role in anti-neuroinflammation via targeting Sp1-mediated multiple inflammatory signaling pathways, which expanded its neuro-protective spectrum as a promising candidate drug.

Overall, our study provided convincing evidence that MA exerted potent anti-neuroinflammatory effect via directly targeting Sp1, thereby inhibiting NF- κ B and MAPK signaling pathways. Our findings indicate that Sp1 may function as crucial target for neuroinflammation therapy and natural product MA may act as a promising drug candidate.

Declaration of Competing Interest

The authors declare that they have no known competing financial interests or personal relationships that could have appeared to influence the work reported in this paper.

Data availability

Data will be made available on request.

Acknowledgments

This study was supported by the National Natural Science Foundation of China (81973199, 81473106, 81773864, 82174008), and the Key Research and Development Project of Shandong Province (2021CXGC010507).

Data availability statement

The raw data supporting the conclusions of this article will be made

available by the authors, without undue reservation.

Ethic statement

The animal protocols were approved by the Institutional Animal Care and Use Committee (IACUC) of Peking University Health Science Center, China (Approval Number: LA2019147).

Author contribution

CHL performed and wrote the manuscript. YZ provided compound murrayafoline A. PFT, KWZ and YJ revised the manuscript, YJ acquired the fundings. All authors read and approved the final manuscript.

Appendix A. Supplementary data

Supplementary data to this article can be found online at <https://doi.org/10.1016/j.bioorg.2022.106178>.

References

- [1] G. Finkenzeller, A. Sparacio, A. Technau, D. Marmé, G. Siemeister, Sp1 recognition sites in the proximal promoter of the human vascular endothelial growth factor gene are essential for platelet-derived growth factor-induced gene expression, *Oncogene* 15 (6) (1997) 669–676, <https://doi.org/10.1038/sj.onc.1201219>.
- [2] G.Z. Yan, E.B. Ziff, Nerve growth factor induces transcription of the p21 WAF1/CIP1 and cyclin D1 genes in PC12 cells by activating the Sp1 transcription factor, *J. Neurosci.* 17 (16) (1997) 6122–6132, <https://doi.org/10.1523/JNEUROSCI.17-16-06122.1997>.
- [3] R.L. Wang, Y. Yang, H. Wang, Y. He, C. Li, MiR-29c protects against inflammation and apoptosis in Parkinson's disease model in vivo and in vitro by targeting SP1, *Clin. Exp. Pharmacol. Physiol.* 47 (3) (2020) 372–382, <https://doi.org/10.1111/1440-1681.13212>.
- [4] H.J. An, H.J. Lee, S. Jang, Y.J. Jung, S.S. Choi, S.C. Park, J.A. Han, Transcription factor Sp1 prevents TRF2(Δ B Δ M)-induced premature senescence in human diploid fibroblasts, *Mol. Cell. Biochem.* 414(1–2) (2016) 201–208, <https://doi.org/10.1007/s11010-016-2672-7>.
- [5] M. Wu, Z.H. Huang, W.F. Huang, M.Y. Lin, W.F. Liu, K.X. Liu, C. Li, MicroRNA-124-3p attenuates myocardial injury in sepsis via modulating SP1/HDAC4/HIF-1 α axis, *Cell Death Discov.* 8 (1) (2022) 40, <https://doi.org/10.1038/s41420-021-00763-y>.
- [6] D.A. Liang, Z.G. Wen, W.L. Han, W.M. Li, L.F. Pan, R.P. Zhang, Curcumin protects against inflammation and lung injury in rats with acute pulmonary embolism with the involvement of microRNA-21/PTEN/NF- κ B axis, *Mol. Cell. Biochem.* 476 (7) (2021) 2823–2835, <https://doi.org/10.1007/s11010-021-04127-z>.
- [7] R. Kekuda, P. Saha, U. Sundaram, Role of Sp1 and HNF1 transcription factors in SGLT1 regulation during chronic intestinal inflammation, *Am. J. Physiol. Gastrointest Liver Physiol.* 294 (6) (2008) G1354–G1361, <https://doi.org/10.1152/ajpgi.00080.2008>.
- [8] G.X. Liu, Y.Q. Li, X.R. Huang, L. Wei, H.Y. Chen, Y.J. Shi, R.L. Heuchel, H.Y. Lan, L. Eisenberg, Disruption of Smad7 promotes ANG II-mediated renal inflammation and fibrosis via Sp1-TGF- β /Smad3-NF- κ B-dependent mechanisms in mice, *PLoS one* 8 (1) (2013) e53573.
- [9] Y. Liu, R.B. Liao, Z.R. Qiang, C. Zhang, Pro-inflammatory cytokine-driven PI3K/Akt/Sp1 signalling and H₂S production facilitates the pathogenesis of severe acute pancreatitis, *Biosci. Rep.* 37(2) (2017) BSR20160483, <https://doi.org/10.1042/BSR20160483>.
- [10] L.i. Song, X.i. Wang, X. Qu, C. Lv, Transcription factor specificity protein 1 regulates inflammation and fibrin deposition in nasal polyps via the regulation of microRNA-125b and the Wnt/ β -catenin signaling pathway, *Inflammation* 45 (3) (2022) 1118–1132.
- [11] L.J. Cai, L. Tu, T. Li, X.L. Yang, Y.P. Ren, R. Gu, Q. Zhang, H. Yao, X. Qu, Q. Wang, J.Y. Tian, Up-regulation of microRNA-375 ameliorates the damage of dopaminergic neurons, reduces oxidative stress and inflammation in Parkinson's disease by inhibiting SP1, *Aging* 12(1) (2020) 672–689, <https://doi.org/10.18632/aging.102649>.
- [12] W. Nong, C.H. Bao, Y.X. Chen, Z.Q. Wei, miR-212-3p attenuates neuroinflammation of rats with Alzheimer's disease via regulating the SP1/BACE1/NLRP3/Caspase-1 signaling pathway, *Bosn. J. Basic Med. Sci.* 10.17305/bjbm.2021.6723. Advance online publication, <https://doi.org/10.17305/bjbm.2021.6723>.
- [13] F. Qin, Y. Zhao, W. Shang, Z.M. Zhao, X. Qian, B.B. Zhang, H. Cai, Sinomenine relieves oxygen and glucose deprivation-induced microglial activation via inhibition of the SP1/miRNA-183-5p/I κ B- α signaling pathway, *Cell. Mol. Biol (Noisy-le-grand)*. 64 (10) (2018) 140–147.
- [14] D.G.I. Kingston, Modern Natural Products Drug Discovery and Its Relevance to Biodiversity Conservation, *J. Nat. Prod.* 74 (3) (2011) 496–511.
- [15] N.E. Thomford, D.A. Senthane, A. Rowe, D. Munro, P. Seele, A. Maroyi, K. Dzobo, Natural Products for Drug Discovery in the 21st Century: Innovations for Novel Drug Discovery, *Int. J. Mol. Sci.* 19(6) (2018)1578, <https://doi.org/10.3390/ijms19061578>.

- [16] T. Nagappan, P. Ramasamy, M.E. Wahid, T.C. Segaran, C.S. Vairappan, Biological activity of carbazole alkaloids and essential oil of *Murraya koenigii* against antibiotic resistant microbes and cancer cell lines, *Molecules* 16 (11) (2011) 9651–9664, <https://doi.org/10.3390/molecules16119651>.
- [17] S.J.N. Tatsimo, J.D.D. Tamokou, M. Lamshöft, LC-MS guided isolation of antibacterial and cytotoxic constituents from *Clausaena anisate*, *Med. Chem. Res.* 24 (2015) 1468–1479, <https://doi.org/10.1007/s00044-014-1233-4>.
- [18] A.C. Adebajo, O.F. Ayoola, E.O. Iwalewa, A.A. Akindahunsi, N.O. Omisore, C. O. Adewunmi, T.K. Adenowo, Anti-trichomonal, biochemical and toxicological activities of methanolic extract and some carbazole alkaloids isolated from the leaves of *Murraya koenigii* growing in Nigeria, *Phytomedicine* 13 (4) (2006) 246–254, <https://doi.org/10.1016/j.phymed.2004.12.002>.
- [19] M. Pieroni, S. Girmay, D. Sun, R. Sahu, B.L. Tekwani, G.T. Tan, Synthesis and structure-activity relationships of lansine analogues as antileishmanial agents, *Chem. Med. Chem.* 7 (11) (2012) 1895–1900, <https://doi.org/10.1002/cmdc.201200346>.
- [20] Y. Nalli, V. Khajuria, S. Gupta, P. Arora, S. Riyaz-Ul-Hassan, Z. Ahmed, A. Ali, Four new carbazole alkaloids from *Murraya koenigii* that display anti-inflammatory and anti-microbial activities, *Org. Biomol. Chem.* 14 (12) (2016) 3322–3332, <https://doi.org/10.1039/c6ob00267f>.
- [21] H.N. Lv, R. Wen, Y. Zhou, K.W. Zeng, J. Li, X.Y. Guo, P.F. Tu, Y. Jiang, Nitrogen oxide inhibitory trimeric and dimeric carbazole alkaloids from *Murraya tetramera*, *J. Nat. Prod.* 78(10) (2015) 2432–2439, <https://doi.org/10.1021/acs.jnatprod.5b00527>.
- [22] Y. Tachibana, H. Kikuzaki, N.H. Lajis, N. Nakatani, Comparison of antioxidative properties of carbazole alkaloids from *Murraya koenigii* leaves, *J. Agric. Food Chem.* 51 (22) (2003) 6461–6467, <https://doi.org/10.1021/jf034700+>.
- [23] Y.Y. Kok, L.Y. Mooi, K. Ahmad, M.A. Sukari, N. Mat, M. Rahmani, A.M. Ali, Antitumour promoting activity and antioxidant properties of girinimbine isolated from the stem bark of *Murraya koenigii* S, *Molecules* 17 (4) (2012) 4651–4660, <https://doi.org/10.3390/molecules17044651>.
- [24] F.N. Ko, Y.S. Lee, T.S. Wu, C.M. Teng, Inhibition of cyclooxygenase activity and increase in platelet cyclic AMP by girinimbine, isolated from *Murraya euchrestifolia*, *Biochem. Pharmacol.* 48(2) (1994) 353–360, [https://doi.org/10.1016/0006-2952\(94\)90107-4](https://doi.org/10.1016/0006-2952(94)90107-4).
- [25] J. Wang, Y. Zheng, T. Efferth, R. Wang, Y. Shen, X. Hao, Indole and carbazole alkaloids from *Glycosmis montana* with weak anti-HIV and cytotoxic activities, *Phytochemistry* 66(6) (2005) 697–701, <https://doi.org/10.1016/j.phytochem.2005.02.003>.
- [26] E.S. Kim, Midostaurin: First Global Approval, *Drugs* 77 (11) (2017) 1251–1259, <https://doi.org/10.1007/s40265-017-0779-0>.
- [27] K. Leung, 1-(9H-Carbazol-4-yloxy)-3-(2-(2-[¹¹C]methoxyphenoxy)ethylamino)-propan-2-ol. Molecular Imaging and Contrast Agent Database (MICAD), National Center for Biotechnology Information (US), 2005.
- [28] Y.M. Chen, N.K. Cao, H.N. Lv, K.W. Zeng, Y.Q. Yuan, X.Y. Guo, M.B. Zhao, P.F. Tu, Y. Jiang, Anti-inflammatory and cytotoxic carbazole alkaloids from *Murraya kwangsiensis*, *Phytochemistry* 170 (2020), 112186, <https://doi.org/10.1016/j.phytochem.2019.112186>.
- [29] N.M. Cuong, H. Wilhelm, A. Porzel, N. Arnold, L. Wessjohann, 1-O-Substituted derivatives of murrayafoline A and their antifungal properties, *Nat. Prod. Res.* 22 (11) (2008) 950–954, <https://doi.org/10.1080/14786410701650212>.
- [30] M. Itoigawa, Y. Kashiwada, C. Ito, H. Furukawa, Y. Tachibana, K.F. Bastow, K.-H. Lee, Antitumor Agents. 203. Carbazole Alkaloid Murrayaquinone A and Related Synthetic Carbazolequinones as Cytotoxic Agents, *J. Nat. Prod.* 63 (7) (2000) 893–897.
- [31] C.B. Cui, S.Y. Yan, B. Cai, X.S. Yao, Carbazole alkaloids as new cell cycle inhibitor and apoptosis inducers from *Clausaena dunniana* Levl, *J. Asian Nat. Prod. Res.* 4 (4) (2002) 233–241, <https://doi.org/10.1080/1028602021000049041>.
- [32] H. Furukawa, T.S. Wu, T. Ohta, C.S. Kuoh, Chemical constituents of *Murraya euchrestifolia* Hayata, *Chem. Pharm. Bull.* 33 (1985) 4132–4138.
- [33] M.H. Pan, C.S. Lai, S. Dushenkov, C.T. Ho, Modulation of inflammatory genes by natural dietary bioactive compounds, *J. Agric. Food Chem.* 57 (11) (2009) 4467–4477, <https://doi.org/10.1021/jf900612n>.
- [34] S. Pathi, I. Jutooru, G. Chadalapaka, V. Nair, S.-O. Lee, S. Safe, A. Ahmad, Aspirin inhibits colon cancer cell and tumor growth and downregulates specificity protein (Sp) transcription factors, *PLoS One* 7 (10) (2012) e48208.
- [35] R.J. Liu, Q. Tan, Q.Q. Luo, Decreased expression level and DNA-binding activity of specificity protein 1 via cyclooxygenase-2 inhibition antagonizes radiation resistance, cell migration and invasion in radiation-resistant lung cancer cells, *Oncol. Lett.* 16 (3) (2018) 3029–3037, <https://doi.org/10.3892/ol.2018.9035>.
- [36] V. Nair, S. Pathi, I. Jutooru, S. Sreevalsan, R. Basha, M. Abdelrahim, I. Samudio, S. Safe, Metformin inhibits pancreatic cancer cell and tumor growth and downregulates Sp transcription factors. *Carcinogenesis* 34(12) (2013) 2870–2879, <https://doi.org/10.1093/carcin/bgt231>.
- [37] I. Jutooru, G. Chadalapaka, S. Sreevalsan, P. Lei, R. Barhoumi, R. Burghardt, S. Safe, Arsenic trioxide downregulates specificity protein (Sp) transcription factors and inhibits bladder cancer cell and tumor growth, *Exp. Cell Res.* 316 (13) (2010) 2174–2188, <https://doi.org/10.1016/j.yexcr.2010.04.027>.
- [38] K.A. Lee, Y.J. Lee, J.O. Ban, Y.J. Lee, S.H. Lee, M.K. Cho, H.S. Nam, J.T. Hong, J.H. Shim, The flavonoid resveratrol suppresses growth of human malignant pleural mesothelioma cells through direct inhibition of specificity protein 1, *Int. J. Mol. Med.* 30(1) (2012) 21–27, <https://doi.org/10.3892/ijmm.2012.978>.
- [39] S. Chintharlapalli, S. Papineni, P. Lei, S. Pathi, S. Safe, Betulinic acid inhibits colon cancer cell and tumor growth and induces proteasome-dependent and independent downregulation of specificity proteins (Sp) transcription factors, *BMC cancer* 11 (2011) 371, <https://doi.org/10.1186/1471-2407-11-371>.
- [40] D.W. Kim, S.M. Ko, Y.J. Jeon, Y.W. Noh, N.J. Choi, S.D. Cho, H.S. Moon, Y.S. Cho, J.C. Shin, S.M. Park, K.S. Seo, J.Y. Choi, J.I. Chae, J.H. Shim, Anti-proliferative effect of honokiol in oral squamous cancer through the regulation of specificity protein 1, *Int. J. Oncol.* 43 (4) (2013) 1103–1110, <https://doi.org/10.3892/ijo.2013.2028>.
- [41] Q. Peng, H. Xu, M. Xiao, L. Wang, The small molecule PSSM0332 disassociates the CRL4ADCAF8 E3 ligase complex to decrease the ubiquitination of NcoR1 and inhibit the inflammatory response in a mouse sepsis-induced myocardial dysfunction model, *Int J Biol Sci.* 16 (15) (2020) 2974–2988. <https://doi.org/10.7150/ijbs.50186>.
- [42] S.J. Lee, K.W. Seo, C.D. Kim, LPS increases 5-LO expression on monocytes via an activation of Akt-Sp1/NF- κ B pathways, *Korean J. Physiol. Pharmacol.* 19 (3) (2015) 263–268, <https://doi.org/10.4196/kjpp.2015.19.3.263>.